

## Photonic crystal slot waveguide absorption spectrometer for on-chip near-infrared spectroscopy of xylene in water

Wei-Cheng Lai, Swapnajt Chakravarty, Xiaolong Wang, Cheyun Lin, and Ray T. Chen

Citation: *Appl. Phys. Lett.* **98**, 023304 (2011); doi: 10.1063/1.3531560

View online: <http://dx.doi.org/10.1063/1.3531560>

View Table of Contents: <http://apl.aip.org/resource/1/APPLAB/v98/i2>

Published by the [American Institute of Physics](#).

---

### Additional information on *Appl. Phys. Lett.*

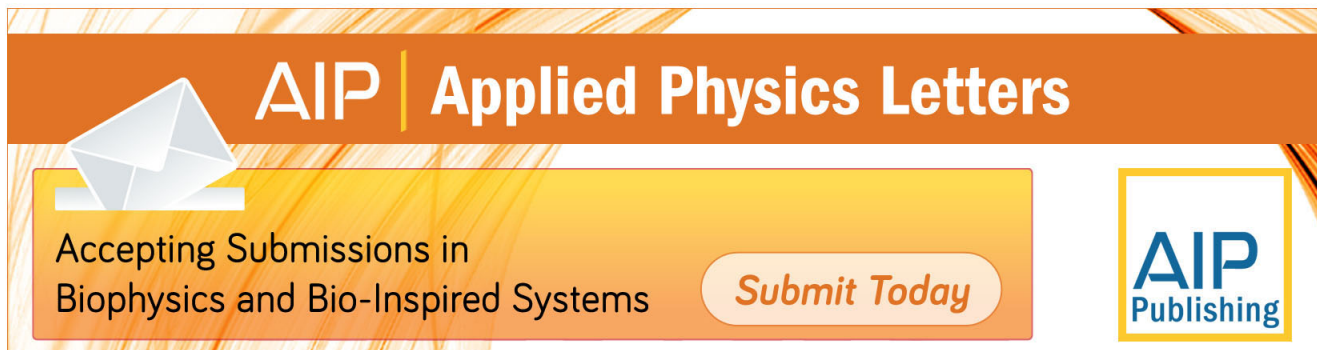
Journal Homepage: <http://apl.aip.org/>

Journal Information: [http://apl.aip.org/about/about\\_the\\_journal](http://apl.aip.org/about/about_the_journal)

Top downloads: [http://apl.aip.org/features/most\\_downloaded](http://apl.aip.org/features/most_downloaded)

Information for Authors: <http://apl.aip.org/authors>

## ADVERTISEMENT



**AIP** | Applied Physics Letters

Accepting Submissions in  
Biophysics and Bio-Inspired Systems

*Submit Today*

**AIP**  
Publishing

# Photonic crystal slot waveguide absorption spectrometer for on-chip near-infrared spectroscopy of xylene in water

Wei-Cheng Lai,<sup>1</sup> Swapnajit Chakravarty,<sup>2,a)</sup> Xiaolong Wang,<sup>2</sup> Cheyun Lin,<sup>1</sup> and Ray T. Chen<sup>1,2,b)</sup>

<sup>1</sup>Department of Electrical and Computer Engineering, University of Texas at Austin, Austin, Texas 78712, USA

<sup>2</sup>Omega Optics Inc., Austin, Texas 78759, USA

(Received 25 September 2010; accepted 4 December 2010; published online 13 January 2011)

We experimentally demonstrate a 300  $\mu\text{m}$  long silicon photonic crystal slot waveguide near-infrared absorption spectrometer. Based on Beer–Lambert absorption law, our on-chip absorption spectrometer combines slow light in a photonic crystal waveguide with a high electric field intensity in a low-index 75 nm wide slot, which effectively increases the optical absorption path length of the analyte. We demonstrate near-infrared absorption spectroscopy of xylene in water, with a polydimethyl siloxane sensing phase for xylene extraction from water. Xylene concentrations up to 100 ppb (parts per billion) (86  $\mu\text{g}/\text{l}$ ) in water were measured. © 2011 American Institute of Physics. [doi:10.1063/1.3531560]

A simple and reliable technique for detection and identification of toxic volatile organic contaminants in water is infrared absorption spectroscopy. Infrared spectroscopy relies on fundamental molecular vibrations and does not require costly analyte labeling, which makes the technique very attractive for sensing and identification compared to other methods. Commercial infrared spectrometers are large, heavy, and expensive. A laboratory-on-chip infrared absorption spectrometer is thus highly desirable for portable and distributed sensing applications.

The principle of infrared absorption spectroscopy is based on Beer–Lambert law. According to this technique, transmitted intensity  $I$  is given by

$$I = I_0 \exp(-\gamma\alpha L), \quad (1)$$

where  $I_0$  is the incident intensity,  $\alpha$  is the absorption coefficient of the medium,  $L$  is the interaction length, and  $\gamma$  is the medium-specific absorption factor determined by dispersion enhanced light-matter interaction. In conventional free-space systems,  $\gamma=1$ ; thus  $L$  must be large to achieve a suitable sensitivity of measured  $I/I_0$ . Although various complex schemes have been demonstrated<sup>1</sup> to increase absorption path lengths,<sup>2</sup> present state-of-the-art dimensions are still significantly large to be accommodated on a chip.

For laboratory-on-chip systems,  $L$  must be small; hence  $\gamma$  must be large. Mortensen and Xiao<sup>3</sup> showed using perturbation theory that

$$\gamma = f \times \frac{c/n}{v_g}, \quad (2)$$

where  $c$  is the velocity of light in free space,  $v_g$  is the group velocity in medium of effective index  $n$ , and  $f$  is the filling factor denoting relative fraction of optical field residing in the analyte medium. Equation (2) shows that slow light propagation (small  $v_g$ ) significantly enhances absorption. Furthermore, the greater the electric field overlap with analyte, the greater the effective absorption by the medium.

Both conditions of small  $v_g$  and high  $f$  are fulfilled in a photonic crystal slot waveguide.

During the past 2 decades, photonic crystal (PC) devices have attracted significant interest due to their unique dispersive properties that allow control and manipulation of light-matter interactions on length scales of the wavelength of light.<sup>4</sup> Various miniature applications have been demonstrated with PC microcavities and PC slot waveguides for light emission,<sup>5</sup> cavity quantum electrodynamics,<sup>6</sup> and electro-optical modulation.<sup>7</sup> PC devices<sup>6</sup> have shown significant promise in sensing applications due to high sensitivity to refractive index changes in the ambient.<sup>8</sup> Change in refractive index of a medium caused by an analyte is, however, not sufficiently analyte-specific and is therefore not a unique signature of the analyte. In contrast, absorption spectrum of an analyte is based on analyte-specific molecular vibrations, and thus identifies the analyte uniquely. In this paper, we demonstrate a PC slot waveguide that enables on-chip optical absorption spectroscopy. We demonstrate near-infrared spectroscopy of xylene in water as a representative contaminant and also due to its environmental and human health significance.

PC waveguides have demonstrated group velocity slow-down factors  $\sim 100$ .<sup>9</sup> Slot waveguides have also demonstrated a significant increase in the electric field intensity in a narrow low-index slot in a high index ridge waveguide, by at least a factor of 10.<sup>10</sup> Slow light in PC waveguides coupled with electric field intensity enhancement in a slot in the PC waveguide can therefore reduce  $v_g$  and enhance  $f$ , thereby theoretically shrinking the required absorption path length by a factor of 1000, an order of magnitude greater than ring resonator devices.<sup>11</sup>

A schematic of our silicon PC slot waveguide device with geometry parameters is shown in Fig. 1(a). The PC waveguide is a W0.8 line defect with uniform lattice constant  $a$ , and width  $0.8 \times \sqrt{3}a$ . The device is coated with a thin  $\sim 8 \mu\text{m}$  film of polydimethyl siloxane (PDMS). PDMS is hydrophobic; hence the use of PDMS ensures that absorption signatures of xylene are obtained without interference from strong near-infrared absorption of water. PDMS cladding

<sup>a)</sup>Electronic mail: swapnajit.chakravarty@omegaoptics.com.

<sup>b)</sup>Electronic mail: raychen@uts.cc.utexas.edu.

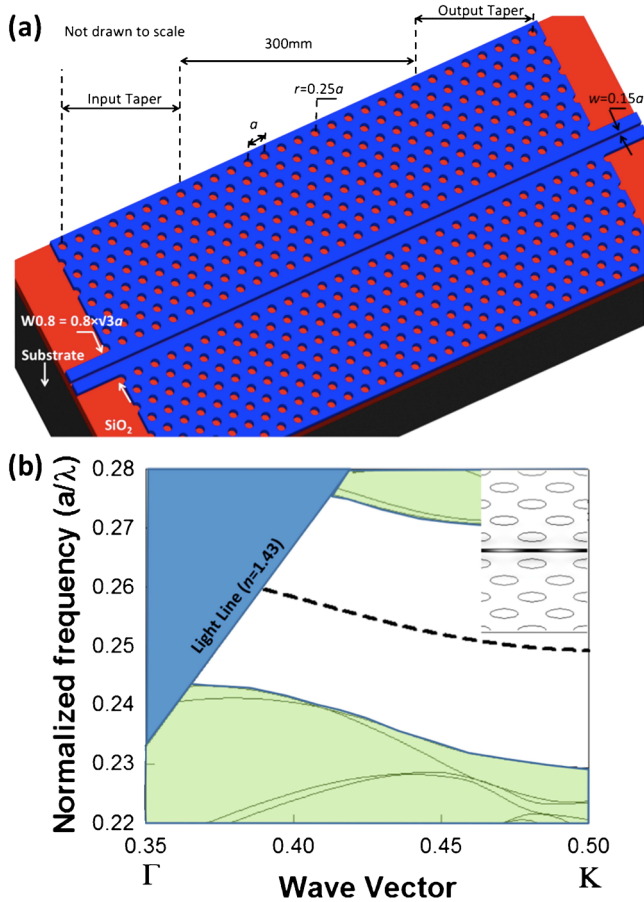


FIG. 1. (Color online) (a) Schematic of a PC slot waveguide device showing different regions. (b) Dispersion diagram of a PC slot waveguide device coated with a PDMS sensing phase. Single mode guided below the light line is shown by dashed curve and mode profile shown in the inset.

thickness chosen avoids interaction between the guided optical mode in the slot and water ambient. The dispersion relation of a defect-guided mode is calculated using a three-dimensional plane-wave expansion method in Fig. 1(b). The design parameters of a W0.8 PC slot waveguide are chosen to support a single PC waveguide slot guided mode. The mode profile of the guided slot mode is shown in the inset. Light is guided into and out of a 300  $\mu\text{m}$  long PC slot waveguide by ridge waveguides using a PC impedance taper where holes adjacent to the PC slot waveguide are shifted in steps by  $0.0025 \times \sqrt{3}a$  over 16 periods to enable gradual change in the group index and thus allow higher coupling efficiency into the slow light guided mode.<sup>12</sup>

Devices were fabricated on a silicon-on-insulator wafer with a 230 nm top silicon layer and 3  $\mu\text{m}$  buried oxide. 45 nm thermal oxide was grown on top of silicon as an etch mask for pattern transfer. PC slot waveguides, tapers, and strip waveguides are patterned in one step with e-beam lithography followed by reactive ion etching. Scanning electron micrograph (SEM) of fabricated structure is shown in Fig. 2. PDMS top cladding was prepared by spinning a 10:1 mixture of Sylgard Elastomer 184 from Dow Corning, New York (refractive index  $n=1.43$ ) and curing agent, followed by oven-baking for 3 h at 90  $^{\circ}\text{C}$ . While electric field enhancement by slot is nearly constant across the entire bandwidth of a guided mode, as observed in the group index simulation in Fig. 3, slow light effects exist over a bandwidth  $\sim 20$  nm. To derive maximum slow light enhancement while

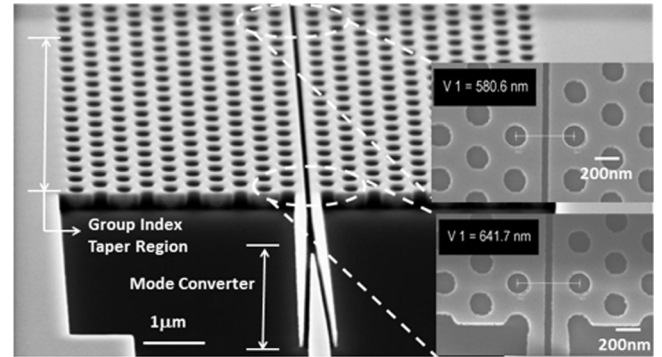


FIG. 2. SEM image of the fabricated W0.8 PC slot waveguide device, before PDMS deposition, showing an input mode converter, an input group index taper, and an etched PC pattern. The insets show the distance between air holes on the two sides of the slot at the beginning and end of the group index taper.

also taking into account coupling efficiencies from a ridge waveguide into a slow light mode due to group velocity mismatch and losses that occur at low group velocities, design parameters are chosen so that group index  $n_g$  of guided mode is  $\sim 40$  at individual xylene absorbance maxima in near-infrared. The absorption signature of xylene in near-infrared extends from 1665 to 1745 nm with absorption peaks at 1674, 1697, and 1720 nm, respectively.<sup>13</sup> Three lattice constants  $a=455$ , 458, and 460 nm are selected for three devices so that slow light propagation occurs at individual absorbance maxima. Devices were tested on a Newport six-axis autoaligning station. Input light from a broadband source (SuperK Versa from NKT Photonics, Denmark) was TE-polarized and butt-coupled to/from the device with polarization maintaining a single mode tapered lensed fiber with mode field diameter  $\sim 3$   $\mu\text{m}$ . Experimental transmission spectrum through a PDMS filled slot in the absence of analyte in Fig. 3 shows that the band edge is red-shifted  $\sim 3$  nm from design (dotted black line). Sample solutions were prepared by transferring 200  $\mu\text{l}$  of xylene into a sealed beaker with 200 ml of de-ionized (DI) water, followed by continuous stirring for 12 h at room temperature, as described in Ref. 14. The entire device is wetted with sample solution, similar to a real environment. Transmitted light was analyzed with an optical spectrum analyzer, in the presence and absence of xylene in water.

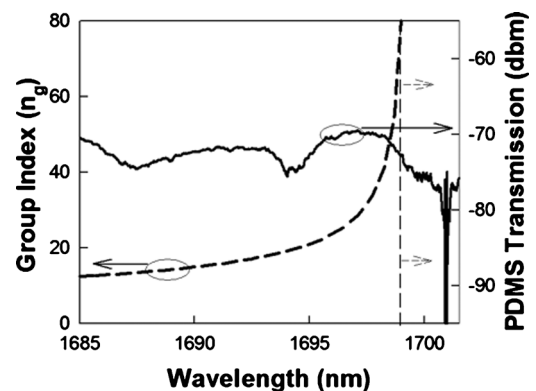


FIG. 3. (Left scale) Group index vs wavelength (dashed curve) as designed with band edge at 1698 nm (dotted black line). (Right scale) Experimental transmission spectrum (solid curve) in a PDMS infiltrated slotted PC waveguide (without analyte), showing band edge shifted in a fabricated device to 1701 nm.

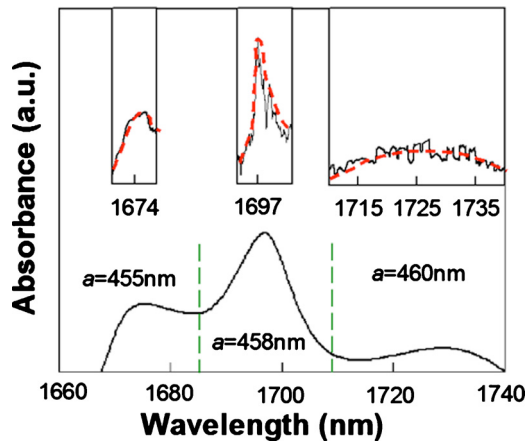


FIG. 4. (Color online) Theoretical spectrum of xylene obtained from Ref. 14 divided into three regions as shown by dotted lines. Experimental transmission spectrum centered on absorbance maxima in each section is plotted in respective insets for 100 ppm (v/v) concentration.

Since PDMS is very thin, the response time is a few seconds. Measurements are performed immediately after analyte introduction. Using Eq. (1), the difference in transmitted intensity through a PDMS clad PC slot waveguide is calculated in the presence and absence of xylene and absorbance of xylene determined. Measurements are performed for all three lattice constants. The theoretical spectrum of xylene<sup>13</sup> is shown in Fig. 4, divided into three sections shown by dotted green lines. An experimentally obtained xylene spectrum is shown for each section, corresponding to individual lattice constants, in the insets of Fig. 4. Good correspondence is observed between experimentally observed absorption peaks and theoretical spectrum.

To determine detection limit, xylene concentration in DI water was varied from  $10^{-5}\%$  or 100 ppb (v/v) to 1% by volume. The intensity of the strongest absorbance peak at 1697 nm is plotted in Fig. 5 as a function of xylene concentration in water. Figure 5 shows that Beer-Lambert law is followed linearly between 100 ppb (v/v) and  $\sim 1$  ppm (parts per million) (v/v); at higher concentrations, absorbance curve deviates from linearity. Detection limit 100 ppb (v/v) ( $\sim 86 \mu\text{g/l}$ ) demonstrated in our 300  $\mu\text{m}$  long device is lower than near-infrared detection limits observed with PDMS disks in water (3 mg/l).<sup>14</sup> The device is more sensitive than methods that require preprocessing for salinity to en-

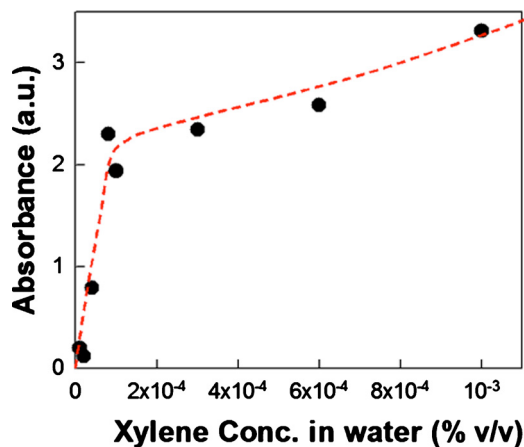


FIG. 5. (Color online) Absorbance magnitude vs xylene concentration in water (%v/v).

hance sensitivity.<sup>15</sup> Our device is more than an order of magnitude smaller in length than PDMS disks above. The detection limit of our device is better than 400  $\mu\text{g/l}$  demonstrated with 11 m optical fibers.<sup>16</sup> Also, the response time in our device is a few seconds compared to  $\sim 60$  min,<sup>15</sup> due to small PDMS thickness for xylene to diffuse. We believe that at the lower end, sensitivity is limited by offset of absorbance peak to  $\sim n_g=20$  due to fabrication errors, as shown in Fig. 3. Detection limit can be enhanced by at least a factor of 3 in current devices in near-infrared by better control of fabrication that positions the band edge closer to peak absorbance as designed. It must be noted that, in midinfrared, 20  $\mu\text{g/l}$  (v/v) detection limit was demonstrated with 50 mm long sample cells.<sup>17</sup> The PC slot waveguide device, based on Maxwell's equations, is readily scalable to midinfrared. Since xylene has approximately two orders larger absorption cross-section in midinfrared, a few hundred parts per trillion (ppt) detection limits are possible in PC slot waveguide devices on 300  $\mu\text{m}$  length scales at longer wavelength. In mixed analyte solutions, multiple PC waveguides can be fabricated simultaneously, each with a different lattice constant, as in the present research to measure absorption spectrum in the corresponding wavelength range, and identifying analytes uniquely by comparing with known infrared absorbance databases.

In summary, we demonstrated a 300  $\mu\text{m}$  long on-chip silicon PC slot waveguide absorption spectrometer that combines slow light with electric field enhancement for near-infrared spectroscopy of xylene in water with detection limit 100 ppb (86  $\mu\text{g/l}$ ). Remote monitoring is enabled by optical fibers; our device is five times more sensitive for xylene in water than existing devices in near-infrared on more than an order of magnitude smaller length scale.

The authors acknowledge the National Science Foundation (NSF) for supporting this work under the SBIR program (Grant No. IIP-0945688).

- <sup>1</sup>M. J. Thorpe, K. D. Moll, R. J. Jones, B. Safdi, and J. Ye, *Science* **311**, 1595 (2006).
- <sup>2</sup>Y. He and B. J. Orr, *Appl. Phys. B: Lasers Opt.* **85**, 355 (2006).
- <sup>3</sup>N. A. Mortensen and S. S. Xiao, *Appl. Phys. Lett.* **90**, 141108 (2007).
- <sup>4</sup>E. Yablonoitch, *Phys. Rev. Lett.* **58**, 2059 (1987); S. John, *ibid.* **58**, 2486 (1987).
- <sup>5</sup>S. Chakravarty, P. Bhattacharya, and Z. Mi, *IEEE Photonics Technol. Lett.* **18**, 2665 (2006).
- <sup>6</sup>T. Yamamoto, M. Notomi, H. Taniyama, E. Kuramochi, Y. Yoshikawa, Y. Torii, and T. Kuga, *Opt. Express* **16**, 13809 (2008).
- <sup>7</sup>C.-Y. Lin, X. Wang, S. Chakravarty, B.-S. Lee, W.-C. Lai, J. Luo, A. K.-Y. Jen, and R. T. Chen, *Appl. Phys. Lett.* **97**, 093304 (2010).
- <sup>8</sup>S. Chakravarty, J. Topofančik, P. Bhattacharya, S. Chakrabarti, Y. Kang, and M. E. Meyerhoff, *Opt. Lett.* **30**, 2578 (2005).
- <sup>9</sup>M. Notomi, *Phys. Rev. Lett.* **87**, 253902 (2001).
- <sup>10</sup>X. Chen, W. Jiang, J. Chen, L. Gu, and R. T. Chen, *Appl. Phys. Lett.* **91**, 091111 (2007).
- <sup>11</sup>A. Nitkowski, L. Chen, and M. Lipson, *Opt. Express* **16**, 11930 (2008).
- <sup>12</sup>X. Wang, S. Chakravarty, B.-S. Lee, C. Lin, and R. T. Chen, *Opt. Lett.* **34**, 3202 (2009).
- <sup>13</sup>D. A. Burns, *Handbook of Near-Infrared Analysis*, 3rd ed. (Taylor & Francis, Hoboken, NJ, 2007).
- <sup>14</sup>J. S. Albuquerque, M. F. Pimentel, V. L. Silva, M. Raimundo, J. J. R. Rohwedder, and C. Pasquini, *Anal. Chem.* **77**, 72 (2005).
- <sup>15</sup>K. M. G. Lima, I. M. Raimundo, and M. F. Pimentel, *Sens. Actuators B* **125**, 229 (2007).
- <sup>16</sup>J. Buerck, S. Roth, K. Kraemer, M. Scholz, and N. Klaas, *J. Hazard. Mater.* **83**, 11 (2001).
- <sup>17</sup>A. M. F. Silva, M. F. Pimentel, I. M. Raimundo, and Y. M. B. Almeida, *Vib. Spectrosc.* **46**, 39 (2008).